

# Expanding 3D DCIP Sensitivity: Applications for Archaean Precious Metal Exploration

Benoit Tournier<sup>1</sup>, Mehran Gharibi<sup>1</sup>, Jeff Warne<sup>1\*</sup>, Ken Tylee<sup>2</sup>

<sup>1</sup>Quantec Geoscience Ltd., 146 Sparks Ave, Toronto, ON, M2H 2S4

<sup>2</sup>McEwen Mining Inc., 2839 Highway 101 East, Matheson, ON, P0K 1N0

## Summary

Employing additional transmits electrodes located in boreholes within the area of investigation for surface 3D DCIP surveys can provide substantial expansion of the region of sensitivity, and increased resolution in areas of interest. The presentation reviews developments required for implementation of the technique and examines results from application for precious metals targets at McEwen Mining's Grey Fox zone located on the Porcupine-Destor deformation zone near Matheson, ON.

## Introduction

The ORION 3D DCIP survey method was developed at Quantec Geoscience Limited in 2010 to provide an omnidirectional DC-IP 3D survey, as a 3D extension of the TITAN 2D DCIP array survey system. The ORION 3D system has the capability to collect data simultaneously across an array of receiver dipoles to provide high-resolution coverage that is suitable for complete 3D imaging of the DC resistivity and IP characteristics of the area surveyed.

ORION 3D Plus complements the surface survey array with current injections located in boreholes. It was briefly introduced at the KEGS Foundation December Mini-Symposium in 2019 with the results of an initial survey for North American Palladium (Warne, Gordon 2019). We present here the results of a more comprehensive survey completed over the Gibson Intrusive at the Black Fox Mine on behalf of McEwen Mining Inc.

## Method

The ORION 3D surface array at Black Fox consisted of a network of 19 acquisition receivers each configured to acquire signal on 6 channels, providing a receiver array of 110 dipoles. The dipole size was 100m.

Data acquisition commenced with the surface DCIP array employing a set of 176 current injection sites distributed along the receiver dipoles (see figure 1).

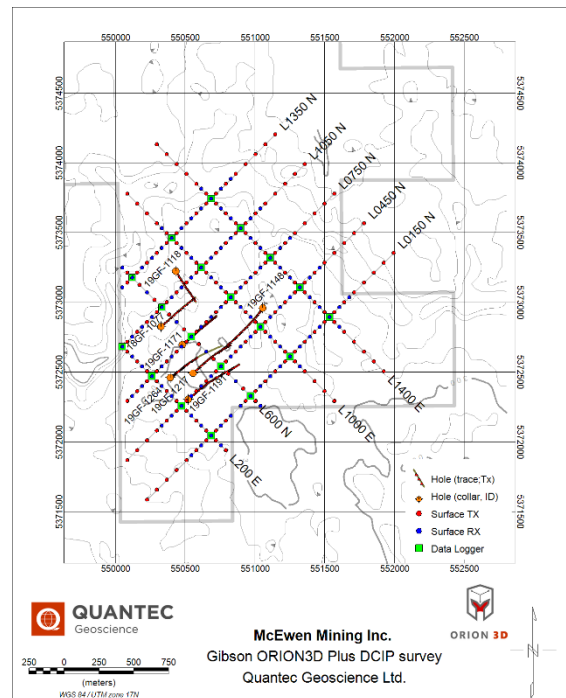


Figure 1: ORION 3D survey array over the Gibson Intrusive.

The surface survey provided a set of approximately 19,000 records (Tx-Rx pairs), but also allowed extraction of 2D data subsets along nine profiles for QC and inversion of DCIP data.

The borehole survey component was then completed along 7 pre-selected boreholes (see figures 1, 2), with length ranging from 500 m to 1 km. A total of 210 current injections were completed located every 20 m along the holes providing approximately 23,000 additional records (Tx-Rx pairs) measured with the same receiver array as in the surface survey.

The DCIP data were collected using a Pole-Dipole layout configuration with a current infinite located 8 km to the south of the grid. The transmitter waveform was a 30/256 Hz square wave at 100% duty cycle. Data at the receiver were sampled continuously at 1 kHz, but windowed for processing according to the transmitter events. The data processing workflow is the same as that applied for TITAN-DCIP data (Sharpe et.al., 2017).

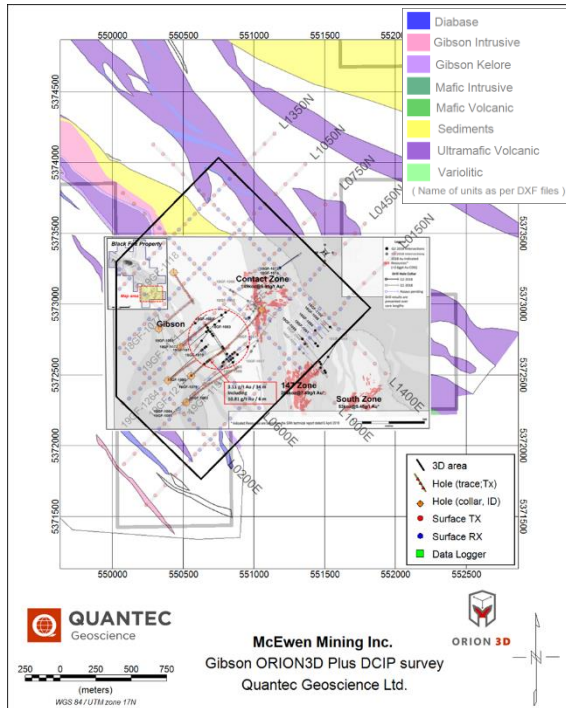


Figure 2: Property geology and boreholes for ORION 3D Plus current injections within the Gibson Intrusive.

Inversions of the surface and borehole datasets were initially performed separately and then together in order to evaluate the impact of each component on the overall inversion results.

The DC and IP data were pre-conditioned individually prior to the inversion to reject outliers and to facilitate the convergence of the optimization process. The error of each data point was adjusted for the inversion process using a general error equation where an error estimate as a percentage of the observed data ( $V_p$  or phase) is added to the estimated data acquisition error and a floor error value. A subset of the total measured data points was then pre-selected based on several criteria related to the measured values (i.e.,  $V_p$  or phase), and their respective observed and calculated errors.

The 3D inversion mesh was designed to cover an area of approximately 2.5 km x 2.3 km. A uniform mesh of 25 m cell size in the X and Y directions was used to cover the receiver array (Figure 3). Padding cells covering ~3 km in each horizontal direction were added to extend the core mesh. The vertical mesh size is fine for the initial 200 m, and then increases in thickness progressively with depth. Surface topography was incorporated into the inversion process to account for terrain variation.

The first output of the analysis is the sensitivity of the models. Figure 4 presents the sensitivity from the 3 type of inversions. The surface results clearly cover the

sub-surface of the area well, but have some depth limitation. The borehole injections extended sensitivity in the regions proximal to their location with additional expansion of the sensitivity resulting from the combination of the data sets.

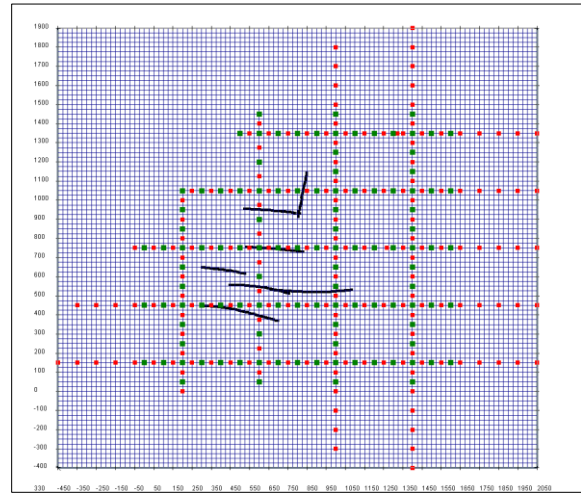


Figure 3: Core mesh for 3D inversion of Gibson Intrusive ORION 3D Plus data sets.

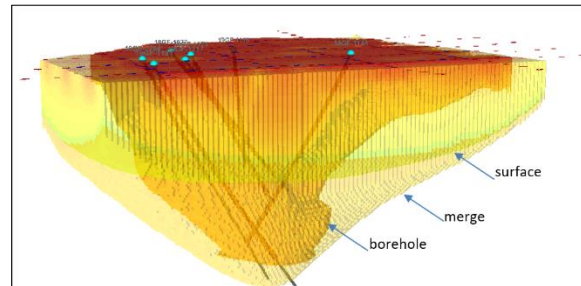


Figure 4: 3D sensitivity (merged, surface, and borehole shapes with different transparency for comparison).

### Examples

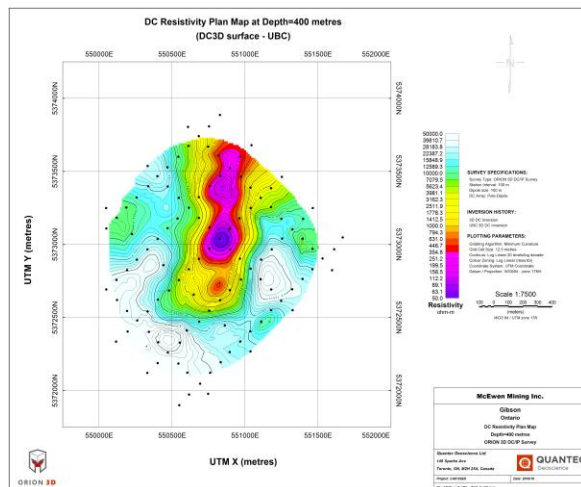


Figure 5: 3D inversion of DC resistivity at 400 m depth, surface data only.

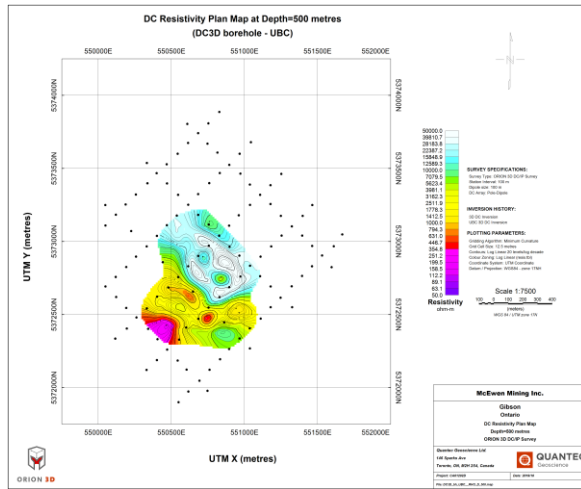


Figure 6: 3D inversion of DC resistivity at 500 m depth, borehole data only.

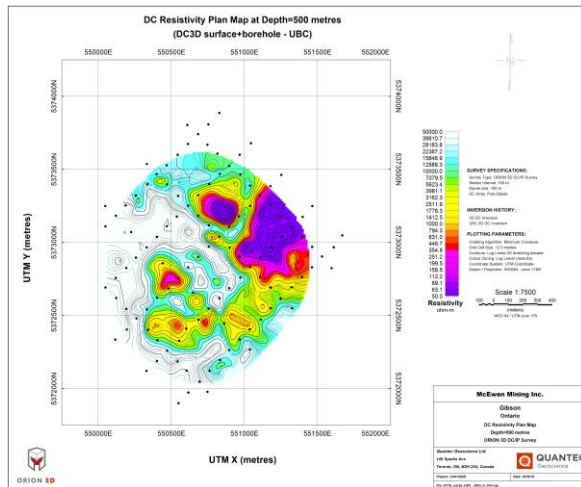


Figure 7: 3D inversion of DC resistivity at 500 m depth, surface plus borehole data.

## Conclusions

Using the boreholes provided good resolution near the boreholes, but sensitivity remained limited away from the holes. The optimum solution is provided by using the combined surface and borehole dataset to provide an increased depth of investigation over the survey area.

As shown in sensitivity plots, resolving structures around the borehole and at larger depth away from the holes and overall success of the surface-borehole combined surveys highly depends on the length of the borehole as well as the distribution of the boreholes, which are the primary factor controlling the capability to increase resolution at depth.

## Acknowledgments

The authors wish to express thanks to McEwen Mining Inc for participating in the further development of the method and permission to publish results.

## References

Gharibi M., et al., 2012. Data redundancy in an omnidirectional 3D DC resistivity dataset. Istanbul International Geophysical Conference and Oil & Gas Exhibition, Istanbul, Turkey, 17-19 September 2012.

Gharibi M., et al., 2012. Full 3D Acquisition and Modelling with the Quantec 3D System - The Hidden Hill Deposit Case Study. 22nd International Geophysical Conference and Exhibition, 26-29 February 2012 - Brisbane, Australia.

Bournas N., and Thomson D., 2013. Delineation of a Porphyry Copper-Gold system using 3D DCIP, CSAMT and MT surveys-Case history, the Santa Cecilia Deposit, Chile. KEGS Symposium 2013 “Copper: Discovery and Delineation”.

McGill D., et al., 2013. Delineating the Kitumba IOCG deposit with the ORION 3D DCIP system. KEGS Symposium 2013 “Copper: Discovery and Delineation”.

McGill D., et al., 2014. Mapping the Junior Lake Area with the Orion 3D DCIP system. SEG Denver 2014 Annual Meeting.

McGill D., and Farquhar-Smith D., 2015. A comparison of 3D DCIP data acquisition methods. ASEG-PESA 2015 – Perth, Australia.

Sharpe, R., et al., 2017. A decade of technological advances in distributed IP & Resistivity. Why it was needed. What was achieved. Exploration17 - Workshop-06: Advances-in-Geophysical-Technology.

Warne J., Gordon R., 2019. Enhancements of 3D Electrical Method Configurations. KEGS Christmas Mini-Symposium 2019